

Development of Inkjet-Printed Doping for Poly-Si Passivating Contacts in Silicon Solar Cells

Jiali Wang¹, Sieu Pheng Phang¹, Christian Samundsett¹, Zhuofeng Li¹, Jie Yang², Zhao Wang², Peiting Zheng², Xinyu Zhang³, Hieu T. Nguyen¹, Josua Stuckelberger¹, Daniel Macdonald¹

¹School of Engineering, The Australian National University (ANU), Canberra, ACT 2601, Australia

²Zhejiang Jinko Solar Co., Ltd, Jiaxing, Zhejiang 314416, China

³Jinko Solar Co., Ltd, 1 Jingke Road, Shangrao, Jiangxi 334100, China

Abstract

We present inkjet printing using phosphorous as the dopant species for the fabrication of high-quality localized polycrystalline silicon (poly-Si) passivating contacts. A detailed study on the impacts of inkjet printer settings, dopant source concentration and annealing temperature on the poly-Si passivating contacts performance was carried out. By applying the optimized process conditions on symmetrical industrially processed intrinsic polycrystalline silicon (i-poly-Si) / SiO_x / n-type crystalline silicon (c-Si) / SiO_x / i-poly-Si substrates, good surface passivation was achieved, reaching directly after annealing at 975 °C an implied open-circuit voltage (*iV_{oc}*) of 699 mV together with a contact resistivity of 6.4 mΩ·cm². After hydrogenation via the deposition of an aluminium oxide (AlO_x) / silicon nitride (SiN_x) stack and subsequent forming gas annealing, the optimum annealing temperature shifted to 950 °C and the *iV_{oc}* further improved to an outstanding value of 729 mV. Optical microscopy and micro-photoluminescence show that a minimum line width of about 50 μm can be achieved after process optimization. Owing to its features of high flexibility, accuracy, safety, low fabrication cost and wide tolerance to chemicals, inkjet printing is a promising technology that can enable the simple fabrication of advanced poly-Si solar cell structures, such as Interdigitated Back Contact (IBC) cells.

Introduction

Polycrystalline silicon (poly-Si) passivating contacts combine an ultrathin SiO_x layer and a doped poly-Si film in a stacked structure, which has proven to significantly reduce carrier recombination at the metal-silicon interface while retaining a low contact resistance [1-3]. By employing this approach to both contacts in an IBC cell structure, a high efficiency of 26.1% has been achieved [4]. Recently, Kiaee *et al.* realized localized poly-Si passivating contacts in a fast and low-cost way, using the inkjet-printed doping technique [8]. In this work, we start from a commercially available phosphorus spin-on-glass (SOG) solution and modify it using glycol to be used as an ink in the printer. We then explore the effects of annealing temperature on the performance of printed poly-Si contacts.

Experimental Details

The experiments were conducted on industrially-prepared symmetric 5 cm × 5 cm i-poly-Si / SiO_x / c-Si / SiO_x / i-poly-Si planar (100) - oriented n-type Cz silicon wafers with a resistivity of 1.5 Ω·cm and a thickness of 150 μm. After a standard cleaning process, the ultrathin SiO_x layer (< 2 nm) was grown by thermal oxidation in a tube at 600 °C for 5 minutes on both sides of the wafers. Subsequently, 100 nm intrinsic poly-Si (i-poly-Si) layers were deposited on the SiO_x layers by low-pressure chemical vapour deposition (LPCVD). The samples were processed up to this stage by Jinko Solar using industrial fabrication tools. After a Radio Corporation of America (RCA) cleaning, the control samples were coated by phosphorus-containing SOG solution (P250, Desert Silicon) on both sides using a spin coater (Laurell WS-650-23NPPB). For the test samples, one side was coated by the spin coater, whereas the other side was doped by the ink using the inkjet printer. The phosphorus containing ink was created using the SOG solution mixed with glycol, with a ratio of 0.75 and 0.9, namely 0.75 ratio solution and 0.9 ratio solution, respectively. Afterwards, a 60-minute-high temperature annealing was carried out under N₂ atmosphere at various temperatures. Thereafter, the phosphorous-silica glasses were removed using 5% hydrofluoric acid (HF). Next, the samples were hydrogenated using forming gas annealing (FGA) at 425 °C for 30 minutes. Subsequently, wafers were subjected to further hydrogenation by depositing stacked layers of Al₂O₃ and SiN_x followed by FGA at 500 °C for 20 minutes. Atomic layer deposition (ALD) and plasma-enhanced chemical vapour deposition (PECVD) were used to deposit Al₂O₃ and SiN_x, respectively. Finally, the stacks were removed by dipping in a buffered HF (BHF; ammonium fluoride (NH₄F) and HF) solution for 7 minutes.

The implied open-circuit voltage (iV_{oc}) was measured by the Photoconductance Decay (PCD) technique with a Sinton WCT-120 lifetime tester [5]. The active dopant profiles were measured after the BHF dip by the electrochemical capacitance-voltage (ECV) method using a WEP Wafer Profiler CVP21. The contact resistivity values were obtained by a Keithley Sourcemeter 2400 using the Cox and Strack method [6], with 300 nm silver circular pads of different diameters evaporated on the front side of the wafer, and 300 nm of silver fully covering the rear side.

Results and Discussion

Figure 1 presents the iV_{oc} values of poly-Si passivating contacts measured after annealing and after hydrogenation via Al_2O_3 / SiN_x stacks. After the annealing processes conducted in N_2 atmosphere, the iV_{oc} values increase initially, reaching the highest values with 699 mV at 975 °C, and then decrease remarkably for anneals at 1000. The subsequent hydrogenation boosts the iV_{oc} values with the highest gain of 81 mV for the wafer printed with 0.9 ratio solution and annealed at 950 °C. Owing to the strong enhancement by hydrogenation, an excellent iV_{oc} of 729 mV is achieved on the sample printed with 0.75 ratio solution annealed at 950 °C. However, for higher temperatures, annealing at 1000 °C, a drop of the iV_{oc} to ~640 mV is observed, and the hydrogenation has only a minor impact. The iV_{oc} trend observed from this experiment bears a resemblance to the results obtained by Ding *et al.*, who adopted the spin-on doping method to fabricate phosphorus doped poly-Si passivating contacts [7].

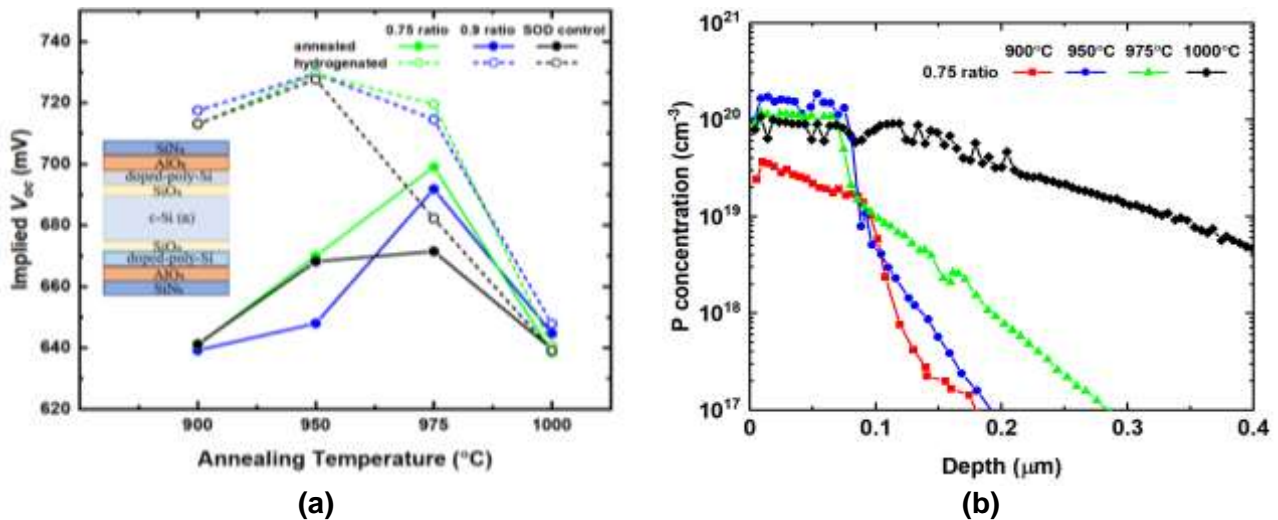


Figure 1(a) iV_{oc} values for phosphorous-doped samples printed by 0.75 and 0.9 ratio solution together with control samples at different annealing temperatures after annealing and after hydrogenation via Al_2O_3 / SiN_x stack. (b) Active dopant concentration for samples printed with 0.75 ratio solution.

By examining the active doping concentration profiles, as shown in Figure 1 (b) for the example of 0.75 ratio, the iV_{oc} variation with annealing temperatures can be explained. Higher temperatures enable more P atoms to diffuse into the c-Si substrate suppressing the minority carrier density near the $SiO_x / c-Si$ interface and reducing the interface carrier recombination [8]. However, when the temperature reaches 975 °C and 1000 °C, the continuous P in-diffusion leads to local disruption of the SiO_x layer and increased Auger recombination within the c-Si bulk [9], thereby a strong decrease in passivation quality occurs which is difficult to passivate by hydrogen. Besides, the doping level in the poly-Si layer increases with the highest concentration at 950 °C before it decreases with higher temperatures. This might imply that the printed glass was depleted at higher temperatures.

A passivating contact should also provide good majority carrier transport. According to Figure 2, the contact resistivities of the fabricated samples remain at a low level below $7 m\Omega \cdot cm^2$ for all annealing temperatures between 950 °C and 1000 °C. This figure excludes the samples annealed at 900 °C, as the I-V curves obtained from the Cox and Strack measurements are nonlinear, which implies a high contact resistivity. So far, the results show that the passivation quality was not sensitive to the solution concentration change between 0.75 and 0.9.

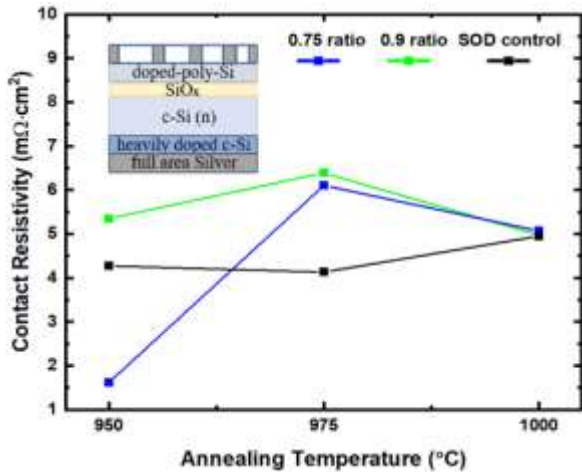
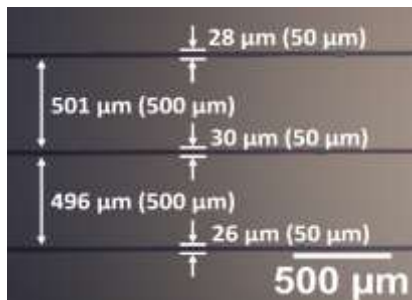
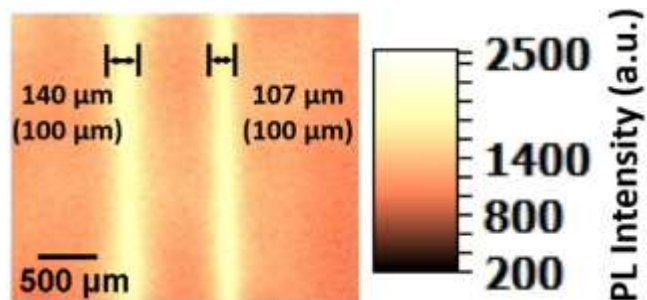


Figure 2. The contact resistivity values of samples after hydrogenation examined using the Cox and Strack method. Note the contact resistivity was measured after the first FGA.

Additionally, the localized performance has been observed via optical microscopy and photoluminescence (PL) imaging with a BT Imaging LIS-R1 system. Figure 3 (a) demonstrates an optical microscope image of lines printed on a mechanically polished 100-orientated bare Si wafer using a 1 pL cartridge and 0.75 ratio solution. The thickness of the printed lines could reach less than 30 μm by using a horizontal drop spacing of 25 μm . Figure 3 (b) is an example PL image showing printed lines on a symmetrical sample after a 1000 $^{\circ}\text{C}$ annealing and a HF dip, where the lines have an intended thickness of 100 μm . The images prove the printer's ability to achieve localized printing, meanwhile, the accuracy of the printing is demonstrated by comparing the measured dimensions and the intended dimensions.



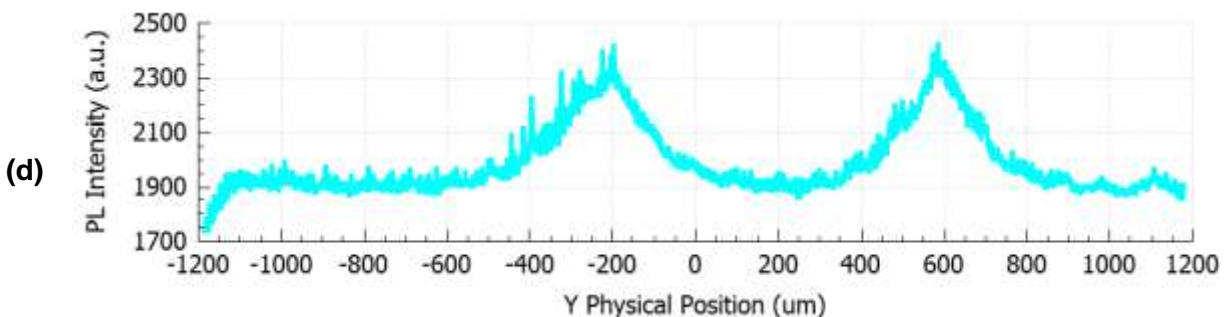
(a)



(b)



(c)



(d)

Figure 3 (a) Optical microscopic image of lines printed by a 1 pL cartridge on a mechanically polished 100-orientated bare Si wafer. **(b)** The PL image of lines printed by a 1 pL cartridge and 0.75 ratio solution the symmetrical sample. The sample was excited at 10 suns and 10 seconds conditions. Note for figure 3 (a) and (b), the measured dimensions are labelled, values in brackets imply the intended dimensions. **(c)** The PL image of the lines in figure 3 (b) with higher resolution

using a hyperspectral PL imager. (d) The PL intensity profile in horizontal direction of figure 3 (c).

Figure 3 (c) is a PL image captured by Photon etc. hyperspectral PL imager (equipped with a microscope objective), which presents the band-to-band PL intensity in the same region as figure 3 (b) with a higher spatial resolution. In addition, the band-to-band PL intensity variation in horizontal direction in figure 3 (c) is further illustrated by figure 3 (d). According to figure (c) and (d), the PL intensity experiences a decrease from the centre of the line and then reaches a stable level at the unprinted region. Two printed lines obtain parallel PL intensity at their centres and share a similar decrement rate of the PL intensity. However, considering that carrier diffusion can lead to significant smearing in such PL images, it is difficult to assess if the blurring evident in the PL images is due to carrier diffusion during measurements, or lateral dopant transport during annealing. Further research is currently underway by conducting and comparing high resolution micro-PL maps and hyperspectral PL imaging, by which the band-to-band emission can be separated from emission from the heavily-doped regions.

Conclusion

We present the development of high-performing n-type poly-Si passivating contacts achieved using the inkjet-printed doping technique. After studying the impact of annealing temperature, we achieved excellent passivation quality with an iV_{oc} of 729 mV in combination with a low contact resistivity below $7 \text{ m}\Omega\cdot\text{cm}^2$ for the case of $950 \text{ }^\circ\text{C}$ annealing temperature and 0.75 ratio solution. Meanwhile, the printer's ability to create localized printing has been proven in-principle, while its performance and accuracy are being further studied.

Reference

- [1] S. W. Glunz and F. Feldmann, "SiO₂ surface passivation layers—a key technology for silicon solar cells," *Solar Energy Materials and Solar Cells*, vol. 185, pp. 260-269, 2018.
- [2] A. Richter *et al.*, "Tunnel oxide passivating electron contacts as full - area rear emitter of high - efficiency p - type silicon solar cells," *Progress in Photovoltaics: Research and Applications*, vol. 26, no. 8, pp. 579-586, 2018.
- [3] A. G. Aberle, "Surface passivation of crystalline silicon solar cells: a review," *Progress in Photovoltaics: Research and Applications*, vol. 8, no. 5, pp. 473-487, 2000.
- [4] F. Haase *et al.*, "Laser contact openings for local poly-Si-metal contacts enabling 26.1%-efficient POLO-IBC solar cells," *Solar Energy Materials and Solar Cells*, vol. 186, pp. 184-193, 2018.
- [5] R. Sinton and A. Cuevas, "Contactless determination of current voltage characteristics and minority carrier lifetimes in semiconductors from quasi-steady-state photoconductance data," *Applied Physics Letters*, vol. 69, pp. 2510-2512, 1996.
- [6] R. H. Cox and H. Strack, "Ohmic contacts for GaAs devices," *Solid-state electronics*, vol. 10, no. 12, pp. 1213-1218, 1967, doi: 10.1016/0038-1101(67)90063-9.
- [7] Z. Ding *et al.*, "Phosphorus-doped polycrystalline silicon passivating contacts via spin-on doping," *Solar Energy Materials and Solar Cells*, vol. 221, p. 110902, 2021.
- [8] Z. Kiaee *et al.*, "Inkjet printing of phosphorus dopant sources for doping poly-silicon in solar cells with passivating contacts," *Solar Energy Materials and Solar Cells*, vol. 222, p. 110926, 2021.
- [9] F. Feldmann, M. Bivour, C. Reichel, M. Hermle, and S. W. Glunz, "Passivated rear contacts for high-efficiency n-type Si solar cells providing high interface passivation quality and excellent transport characteristics," *Solar energy materials and solar cells*, vol. 120, pp. 270-274, 2014.